Optimization of Photocatalytic Reduction of Cr(VI) in Water with Nano ZnO/Todorokite as a Catalyst: Using Taguchi Experimental Design

Sabonian, Mayam; Mahanpoor, Kazem*[+]

Department of Chemistry, Arak Branch, Islamic Azad University, Arak, I.R. IRAN

ABSTRACT: *In the present work, the solid state dispersion method has been used to stabilize ZnO on Todorokite (TD). ZnO/TD catalysts have been characterized by SEM and XRD. Optimum process conditions were determined for the removal of Cr(VI) from water using the Taguchi fractional design method. Four controllable factors containing pH, photocatalyst amount, irradiation intensity and initial concentration of Cr(VI) at three levels were identified for each factor. The optimum conditions were found to be as follows pH= 2, photocatalyst amount= 100 mg/L, irradiation intensity= 7.63 W/m^2 and Cr(VI) concentrations= 15 ppm. In optimum conditions a first order reaction to k= 0.1492 min^{-1} was observed in the photocatalytic reduction of Cr(VI) in water by UV/ZnO/TD.*

KEYWORDS: *ZnO/TD; Photocatalytic-reduction; Taguchi; Cr(VI).*

INTRODUCTION

Cr(VI) exhibits considerable toxic activity in most organics, being carcinogenic in humans and animals. Cr(VI) is a toxic pollutant found in the wastewater of metallurgic, electronic, textile and tanning [1-5]. Cr exists to two common oxidation states, Cr(III) and Cr(VI). The Cr(VI) is five hundred times more toxic than the Cr(III) [6]. The toxic effects of Cr(VI) include skin irritation, lung cancer and harmful effects on kidney, liver and gastric [7, 8]. Conventional methods of Cr(VI) removal includes ion exchange, chemical reduction, adsorption on absorptive materials such as zeolite or active carbon, microorganism reduction and photocatalytic reduction [9, 10]. Photocatalytic procedure is important and practical method of removal of Cr(VI) from aqueous solution. Photocatalytic methods take based on the mechanism of electron-hole [11, 12]. By radiation, electron transfer from the valence band of the conduction band. Electrons in the conduction band can be reduced hexavalent form to the trivalent form. The photocatalytic reduction of Cr(VI) was done with TiO_2, ZnO, CdS and WO_3 semiconductors [13, 14].

In order to optimize photocatalytic reduction process, it is essential to study all factors influencing the process. Studying the effects of individual factors of the process is difficult and time-consuming, especially if these factors are not independent and have an interactive effect. Employing experimental design could eliminate these problems. The interaction effects of different factors could be attained using Design of Experiments (DoEs) such as Taguchi. This method could reduce the total

* *To whom correspondence should be addressed.*

+ E-mail: k-mahanpoor@iau-arak.ac.ir

1021-9986/2019/6/105-113 9/$/5.09

number of experiments by optimizing all the affecting factors [15].

ZnO, the most stable oxide under ambient conditions, is widely used in catalysts, sensors, water treatment [16]. Optical band gap in Zinc oxide is 3.37ev. Then, ZnO is semiconductor with high photocatalytic property. Other properties of Zinc oxide, such as, insolubility in water, high chemical stability, non-toxic and low cost are suitable for the photocatalytic reduction process. [17,18].

Transition metals are well known as the active species in many artificial catalytical systems, the transition-metal based Octahedral Molecular Sieve (OMS) promises a simpler and more effective incorporation of various other transition metal active species. Octahedral coordinated porous manganese oxide materials have attracted a great deal of attention due to their controllable structures, porosities, and catalytical selectivity in relation to those of tetrahedral porous materials. These superior advantages have raised many useful applications of manganese oxide OMS in catalysis, semiconductors, ion-exchange, radioactive hazard separation, sensors, and batteries.

Todorokite is one kind of manganese oxide. Todorokite is mined as an ore of manganese. Todorokite is made up of ($Mn^{4+}O_6$) octahedral that share edges to form triple chains. These chains share corners to form roughly square tunnels. The unit cell has six manganese Mn^{4+} sites and twelve oxygen O^{2-} sites constituting the octahedral framework. The tunnels contain large cations and water molecules.

Studies have shown that Todorokite exhibits dehydration and cation-exchange behavior similar to many zeolites suggesting possible potential as a base of catalyst [19]. Photocatalytic property is strongly dependent on the transport of photo-generated electrons and holes in the photocatalysts. Free electrons and holes (free charge carriers) can be scattered by various kinds of random defects [20-22].

The separation of photogenerated electrons and holes will facilitate the photocatalytic reduction process. There is a wide range of applications of Taguchi method, from engineering and agriculture to chemistry [23-27]. The using of the Taguchi method of the ordinary experimental design methods, in addition to keeping the experimental cost at a lower level, is that it minimizes the product diversity response. Another benefit is that optimal experimental conditions can be used in the real environment [27]. In the present work is stabilized ZnO/TD. The solid state dispersion method has been used to stabilize ZnO on Todorokite. This study was determined optimum process conditions for the reduction of Cr(VI) from water using the Taguchi fractional design method. The variable used in the optimization are, pH, photocatalyst amount, irradiation intensity and Cr(VI) concentrations. The four parameters were set at three levels to observe the main effects.

EXPERIMENTAL SECTION

Materials

All materials containing: Potassium dichromate ($K_2Cr_2O_7$), Sulfuric acid (H_2SO_4) and Sodium hydroxide (NaOH), Manganese (II) chloride tetrahydrate ($MnCl_2 \cdot 4H_2O$), Magnesium sulfate heptahydrate ($MgSO_4 \cdot 7H_2O$), Potassium persulfate ($K_2S_2O_8$), Urea ($CO(NH_2)_2$) and Zinc nitrate hexahydrate ($Zn(NO_3)_2 .6\ H_2O$).

Procedure

Catalyst production Procedure

Todorokite synthesized by the hydrothermal method based on previous research [28]. A 6.0 M NaOH solution (30 ml) was added as a drip for 15 min to a $MnCl_2$ solution, which was prepared by the dissolution of 1.98 g of crystalline hydrate in 15 ml of distilled water. Then, 1.89 g $K_2S_2O_8$ and 0.344 g $MgSO_4 \cdot 7H_2O$ were added for 30 min to the formed yellow precipitate of manganese hydroxide (II). The precipitate was mixed with 200 mL of $MgSO_4$ solution (1.0 M) for 12 h. The product was subjected to a hydrothermal treatment of the hermetic Teflon cell filled with distilled water 75–85% by volume. One steel autoclave with the Teflon cell was put into an electric furnace at 160 °C to 24 h. When the experiment was over, the autoclave was removed from the furnace and cool down to room temperature for 8–12 h. Then the Mg Todorokite crystalline precipitates were repeatedly washed with distilled water until the absence of any reaction to Cl^-. H-Todorokite was obtained by holding Mg-Todorokite in the 1.0 M HNO_3 solution for 48 h, under mixing of a suspension with a magnetic mixer. The precipitate was washed with distilled water until pH= 7.

2 g of Todorokite powders added to 25 ml of 5.0 M zinc nitrate and then was placed on the heater stirred for 2 hours. Then 25 ml of 2.0 M urea solution to a temperature

of 90-95 °C was added to the mixture and put in a water bath for 6 hours. The mixture was passed through filter paper. Precipitates were dried at ambient temperature. Sediment was placed in a furnace at 350 °C for 3 hours.

General procedure

An MDF box was designed in which a batch Pyrex reactor with 300 ml capacities were placed. On the upper section of the box, three mercury lamps (Philips 15W) were built-in as UV light sources. The radiation is generated almost exclusively at 254 nm. These lamps were set at the same intervals, so that the light was evenly emitted at the liquid surface inside the reactor. To measure the radiation intensity used by the Hagner EC1-X Lux Meter device.

The liquid inside the reactor was agitated by magnetic stirrer. In order to carry out each experiment (according to Table 2), 250 ml Cr(VI) solution was (with specified concentration) poured inside the reactor. The specified amount of photocatalyst (With specific pH) was added to the reactor. In all experiments, pH adjustment was done via minimum use of H_2SO_4 and NaOH. Then, stirrer and UV lamps were turned on to initiate the process. Sampling was done every 10 min (by a 5 ml syringe,). In order to fully separate the catalyst from solution, the samples were centrifuged for 3 min with 3500 rpm speeds. The Cr(VI) concentration of the samples was determined using a UV/Vis spectrophotometer at λ_{max}= 350 nm. The percent of photoreduction efficiency as a function of time is given by:

$$\text{Cr reduction\% (x\%)} = [(A_0 - A)/A_0] \times 100 \quad (1)$$

Where A_0 and A are the Absorption of Cr(VI) solution at λ_{max}= 350 in t=0 and t, respectively. For the determination of optimal condition used Taguchi experimental design. This method includes the following steps:

1 - The variables affecting the test results will be determined

2 - Levels of each variable is identified separately (interaction between variables to be considered) 3 - choose the suitable orthogonal array (OA) and the assignment of process parameters to the orthogonal array 4 - Required experiments are performed based on the (OA)

5 - Calculate the performance statistics

6 - Experimental result analysis is done using ANOVA statistics and performance;

Taguchi experimental design (with Qualitek-4 software) used for determination of optimal condition. Effect of experimental factors on the photocatalytic reduction of Cr(VI) and their levels are given in Table 1.

The orthogonal array experimental design method was selected to determine an experimental plan, as seen in Table 2 [27].

In order to see the effects of noise sources, reduction Cr(VI), each test repeated three times at the same conditions. Optimize function statistics were chosen as indicators. Three classes of function statistics, bigger are better, smaller is better and nominal is the better. In this research, the function statistics bigger is the better was used to define the optimal conditions [27].

The bigger are better function statistics was given by Eq. (2).

$$SN_L = -10\log\left(\frac{1}{n}\sum_{i=1}^{n}\frac{1}{Y_i^2}\right) \quad (2)$$

Where SNs are function statistics, and the number of repetitions done for an experimental combination, and *Yi* the function value of it experiment.

In the Taguchi Experiment design method, the experiment corresponding to optimum experimental conditions might not have been done during the all-time of the experimental stage. In such cases, the function amount corresponding to optimum test conditions can be predicted by utilizing the balanced characteristic of OA. For this, the additive model may be used Eq. (3) [23]:

$$Y_i = \mu + X_i + e_i \quad (3)$$

Where μ is the overall mean of performance value; X_i the fixed effect of the parameter level combination used in it experiment and e_i the random error in it experiment.

RESULT AND DISCUSSION

Characterization of photocatalyst

The SEM images of ZnO particles have loaded onto the surface of Todorokite shown in Fig. 1. It seems that the ZnO oxide particle takes place on the surface of Todorokite. All surfaces of Todorokite have not covered with ZnO, so Cr(VI) pollutants can be absorbed on the surface of the Todorokite.

Table 1: Experimental parameters and their levels.

Factors	Level 1	Level 2	Level 3
A) pH	2	3	4
B) Cr(VI) concentration (ppm)	15	20	25
C) Catalyst amount (mg/L)	50	75	100
D) Irradiation intensity (W/m^2)	2.82	5.18	7.63

Table 2: Experimental plan table.

Experimental number	Initial concentration of Cr(VI) (mg/L)	Solution pH	Dosage of ZnO/TD Nano catalyst (mg/L)	Radiation intensity (W/m^2)
1	1	1	1	1
2	1	2	2	2
3	1	3	3	3
4	2	1	2	3
5	2	2	3	1
6	2	3	1	2
7	3	1	3	2
8	3	2	1	3
9	3	3	2	1

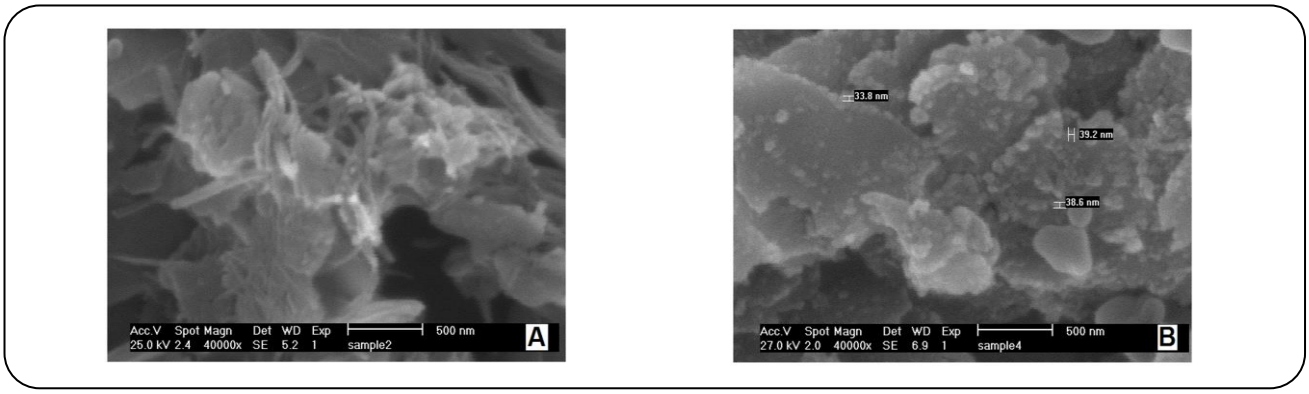

Fig. 1: SEM image of ZnO/Todorokite prepared by SSD method.

To reveal the interaction between the ZnO and the TD, the crystal structures of the raw TD and the ZnO/TD calcined at the 400 °C after 5 h was measured, as shown in Fig. 2. It is clear that the XRD patterns of ZnO/TD consist of the raw TD very well as calcined at 400 °C for 5 h. It implies that the frame structure of TD after ZnO loading has not been destructed.

Determination of optimum operational parameter on the photoreduction of Cr(VI)

The photocatalytic reduction of Cr(VI) from the synthetic effluents was studied in different experimental conditions (according Table 1 and 2). To determine the optimum conditions for the reduction of Cr(VI) in the solutions, were investigated the effects of operational parameter (Cr(VI) concentrations, catalyst amount, pH and irradiation intensity). The reaction conditions in which the effect of the parameters investigated and the experimental results are given in Table 3. The degrees of the influences of parameters on the performance statistics are given in the graphs in Figs. 3-6.

The numerical value of the maximum point in each graph is the best value of factor.

Table 3: Experimental result of an orthogonal array of L_9 .

Exp No	X_1(%)	X_2(%)	X_3(%)	Average
1	98.76	97.74	99.75	95.75
2	55.98	55.42	56.54	55.98
3	38.66	38.41	38.91	38.66
4	77.03	76.26	77.8	77.03
5	48.13	47.65	48.62	48.13
6	12.99	12.86	13.12	12.99
7	75.77	75.11	76.53	75.80
8	45.43	45.13	45.72	45.42
9	8.89	8.8	8.98	8.89

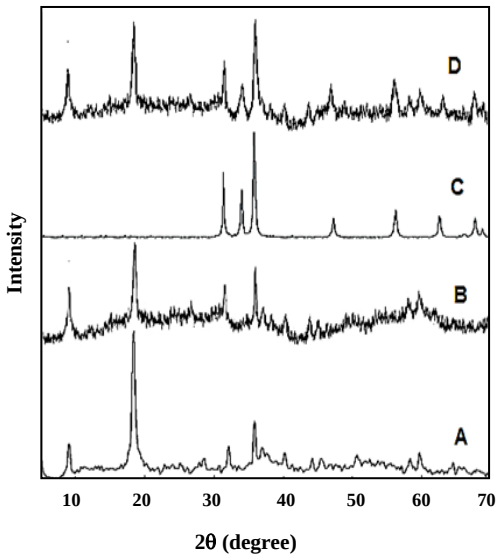

Fig. 2: X-ray diffractogram of the synthesized Todorokite [28] (A), synthesized Todorokite (B), ZnO [29] (C) and synthesized ZnO/Todorokite (D).

The reduction of the Cr(VI) has decreased with increasing Cr(VI) concentration (As shown in Fig. 3). With increasing concentrations of potassium dichromate, absorption light beams in the solution increases. For this reason, the light that can reach the catalyst surface is reduced. Therefore, the removal process efficiency decreased [30].

Under UV irradiation, electron–hole pairs generated at the surface of ZnO/TD NPs. After the separation of the electron–hole pairs, the electrons reduced Cr(VI) to Cr(III), the holes might lead to the generation of O_2 in the absence of organics [31].

$$ZnO/TD \longrightarrow ZnO/TD\ (e^-/h^+) \quad (4)$$

$$Cr_2O_7^{2-} + 14H^+ + 6e^- \longrightarrow 2Cr^{3+} + 7H_2O \quad (5)$$

(In acidic solutions)

$$Cr_2O_7^{2-} + 7H_2O + 6e^- \longrightarrow 2Cr(OH)_3 + 8OH^- \quad (6)$$

$$2H_2O + 2h^+ \longrightarrow H_2O_2 + 2H^+ \quad (7)$$

In addition, H_2O_2 can reacted with Cr(VI) as a following:

$$Cr_2O_7^{2-} + 3H_2O_2 + 8H^+ \longrightarrow 2Cr^{3+} + 7H_2O + 3O_2 \quad (8)$$

However, for more concentrated solutions, more irradiation time is needed in order to fully reduction of Cr(VI) in the solution. This might be due to the fact that the increased concentration of the Cr(VI) has inhibiting effects on direct contact and reaction between Cr(VI) and electrons in conduct bond; because more Cr(VI) ions will be adsorbed onto the surface of the catalyst.

That the electron in conduct bond is available for the reaction to the Cr(VI) absorbed on the surface of TD. As shown in Fig. 4 is the increasing amount photocatalytic reaction rate increases because it increases the speed formation of electron in conduct bond that formed under UV radiation.

Photocatalytic reduction of Cr(VI) better done an acidic solution (as shown in Fig. 5). Because reduction reaction to acidic solution was done very well. (in the reactions 5 and 8).

Furthermore, electrons in the conduction bond (e^-_{CB}) of catalyst surface can reduce molecular oxygen to superoxide anion (Eq. (9)). [32]

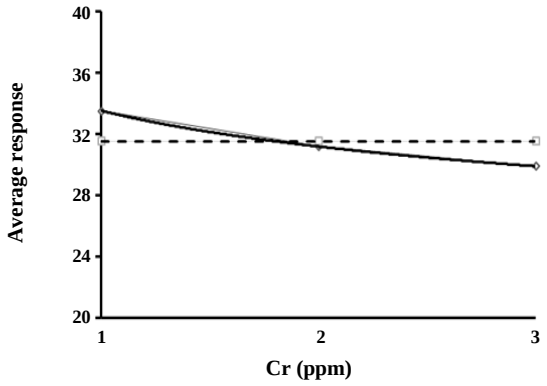

Fig. 3: Effect of Cr(VI) level in photoreduction of Cr(VI).

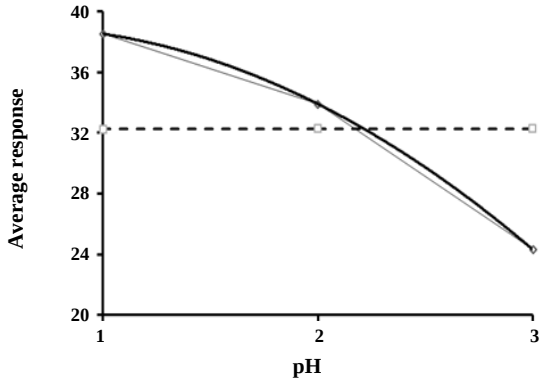

Fig. 5: Effect of pH level in photoreduction of Cr(VI).

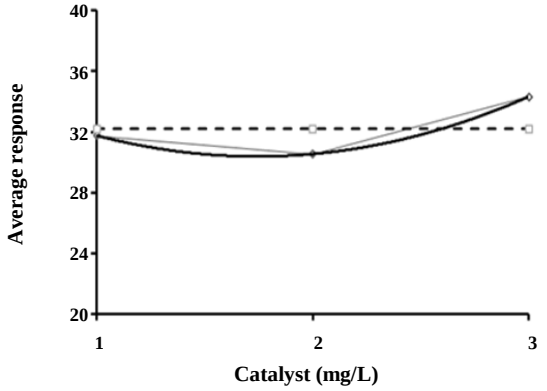

Fig. 4: Effect of photocatalyst level in photoreduction of Cr(VI).

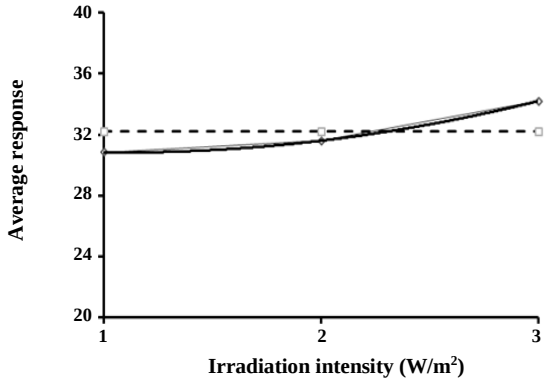

Fig. 6: Effect of irradiation intensity in photoreduction of Cr(VI).

$$e^-_{CB} + O_2 \longrightarrow O_2^{\bullet-} \quad (9)$$

Correspondingly, H_2O_2 is formed by $O_2^{\bullet-}$ in acidic solution:

$$O_2^{\bullet-} + H^+ \longrightarrow HO_2^{\bullet} \quad (10)$$

$$HO_2^{\bullet} + HO_2^{\bullet} \longrightarrow H_2O_2 + O_2 \quad (11)$$

$$O_2^{\bullet-} + HO_2^{\bullet} \longrightarrow HO_2^- + O_2 \quad (12)$$

$$HO_2^- + H^+ \longrightarrow H_2O_2 \quad (13)$$

Therefore, the pair of hydrogen peroxide and oxygen is formed by reactions of 10 to 13 in acidic solution. According to reaction 8, Cr(VI) reduces by Hydrogen peroxide.

As seen in Fig. 6, the reduction rate increased when the irradiation intensity changed from 1 to 3. Band-gap sensitization mechanism does not have any influence on the photocatalytic reduction rate or mechanism. However, various studies have revealed that with an increasing light intensity, the rate of photocatalytic reduction increases. As the intensity of radiation increases, the number of holes and electrons increases. Based on the reaction mechanism, the speed of the chromium reduction reactions increases with the increase in the number of electron - hole pairs.

As shown in Fig. 7 has been formed based on Taguchi experiment design the most effective parameter on the photocatalytic decomposition of Cr(VI) is pH. Defined in Fig. 8 is the effect of each of the variables pH, irradiation intensity, photocatalyst amount and Cr(VI) concentration on other variables. Based on the results of interaction of catalyst and irradiation intensity with each other is the highest value. These results demonstrated that both UV light and a photocatalyst were needed for the effective reduction of Cr(VI). It was shown that the photocatalytic reduction of Cr(VI) in solution is initiated by photoexcitation of the semiconductor, followed by the formation of an electron-hole pair on the surface of the catalyst (Eq. (1)).

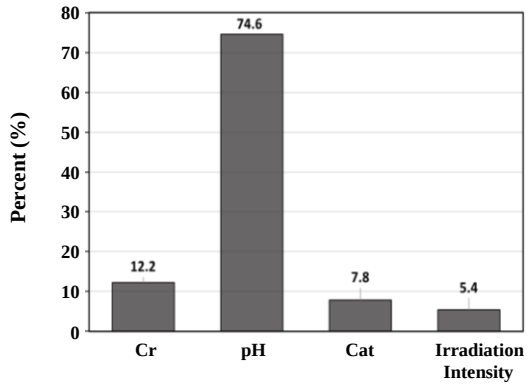

Fig. 7: Effect of parameters on photocatalytic reduction of Cr(VI).

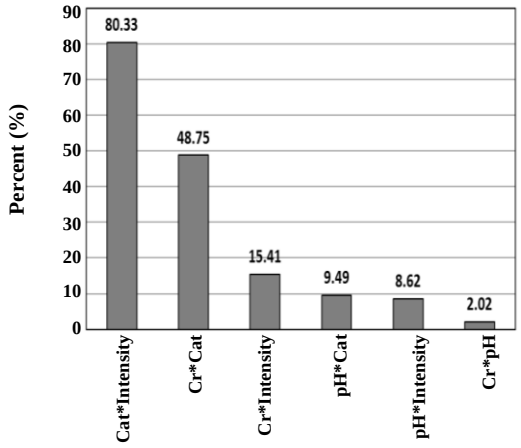

Fig. 8: Effect of each parameter on other variables.

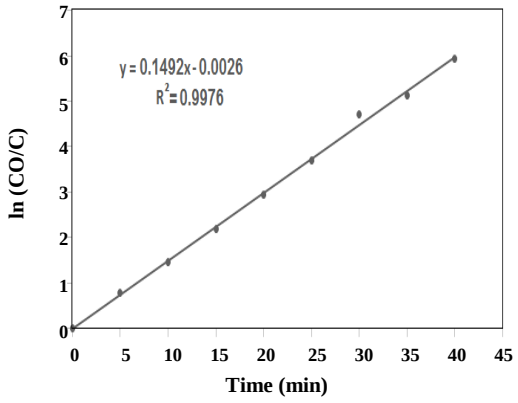

Fig. 9: Kinetic plot of pseudo-first order photocatalytic degradation of Cr(VI) in optimal condition. (pH= 2, photocatalyst amount= 100 (mg/L), Irradiation intensity = 7.63 W/m^2 and initial Cr(VI) concentration= 15 ppm).

For determining the optimum conditions and the share of each parameter involved, the methods of averaging and drawing graphs were used. In Figs. 3-6, the average response for each parameter are displayed. The results, based on average indicate that the optimum condition for the initial concentration of Cr (VI) is level 1 (15 ppm), the dosage of nanocatalyst is level 3 (100 mg/L), the pH of the solution is level 1 (2) and the intensity of irradiation y is level 3 (7.63 W/m^2). Because, the performance statistics of ''the bigger – the better'' was used to define the optimum conditions.

Kinetics of Photocatalytic reduction of Cr(VI)

Kinetic of photocatalytic reduction of Cr(VI) shows good match with pseudo-first-order kinetic of heterogeneous reaction models. In the batch system, kinetic integral equation of pseudo-first-order relationship between concentration (C) and time (t) is as follows [33]:

$$\ln\left(\frac{C_0}{C}\right) = k_{app}t \qquad (14)$$

Where C_0 and C are Cr(VI) initial concentration and Cr(VI) concentration after the specified time, respectively, k_{app} is the apparent pseudo-first-order rate constant and t is the photocatalytic reaction time. Plot of ln (A_0/A) versus t for optimal condition of photocatalytic reduction of Cr(VI) is shown in Fig. 9.

CONCLUSIONS

Physical and chemical characterization of supported photocatalyst were determined by SEM and XRD techniques. According to the literature, the results demonstrated that produced ZnO/TD has sufficient properties as a photocatalyst for reduction of Cr(VI). Here, a Taguchi design method was used for optimization of the parameter values for obtaining desired characteristics. The various factors affecting the reduction process were analyzed and optimized pH, the irradiation intensity has been shown to be highly influential upon the photocatalytic reduction of Cr(VI). In optimal conditions (pH= 2, photocatalyst amount= 100 mg/L, irradiation intensity = 7.63 W/m^2 and initial Cr(VI) concentration= 15 ppm) that analyzed by Taguchi method, determined kinetics of the photocatalytic reduction reaction. Pseudo-first-order model reaction good match with empirical data of photocatalytic reduction of Cr(VI) reaction.

Acknowledgment

The authors would like to gratefully acknowledge the members of the Research Laboratory of Islamic Azad University, Arak branch, Arak, Iran.

Received : Jul. 8, 2018 ; Accepted : Oct. 8, 2018

REFERENCES

[1] Khalil L.B., Mourad W.E., Rophael M.W., Photocatalytic Reduction of Environmental Pollutant Cr(VI) over Some Semiconductors under UV/Visible Light Illumination. *Appl. Catal., B,* **17**: 267-273 (1998).

[2] Riahi Samani M., Borghei S.M., Olad A., Chaichi M.J., Influence of Polyaniline Synthesis Conditions on its Capability for Removal and Recovery of Chromium from Aqueous Solution. *Iran. J. Chem. Chem. Eng. (IJCCE),* **30**: 97-100 (2011).

[3] Fu H., Lu G., Li S., Adsorption and Photo-Induced Reduction of Cr(VI) Ion in Cr(VI)-4CP (4-Chlorophenol) Aqueous System in the Presence of TiO_2 as Photocatalyst. *J. Photochem. Photobiol., A,* **114**: 81-88 (1998).

[4] Alaa M., Osman T.A., Toprak M.S., Muhammed M., Yilmaz Eda., Uheida A., Visible Light Photocatalytic Reduction of Cr(VI) by Surface Modified CNT/Titanium Dioxide Composites Nanofibers, *J. Mol. Catal. A: Chem.*, **424**: 45-53 (2016).

[5] Litter M.I., Heterogeneous Photocatalysis: Transition Metal Ions in Photocatalytic Systems, *Appl. Catal., B,* **23**: 89-114 (1999).

[6] Gupta V., Rastogi A., Nayak A., Adsorption Studies on the Removal of Hexavalent Chromium from Aqueous Solution Using a Low Cost Fertilizer Industry Waste Material, *J. Colloid Interface Sci.,* **342**: 135-141 (2010).

[7] Gupta S., Babu B.V., Modeling, Simulation, and Experimental Validation for Continuous Cr(VI) Removal from Aqueous Solutions Using Sawdust as an Adsorbent. *Bioresour. Technol.,* **100**: 5633-5640 (2009).

[8] Yoon J., Shim E., Bae S., Joo H., Application of Immobilized Nanotubular TiO_2 Electrode for Photocatalytic Hydrogen Evolution: Reduction of Hexavalent Chromium (Cr(VI)) in Water, *J. Hazard. Mater.*, **161**: 1069-1074 (2009).

[9] Golder A.K., Chanda A.K., Samanta A.N., Ray S., Removal of Hexavalent Chromium by Electrochemical Reduction-Precipitation: Investigation of Process Performance and Reaction Stoichiometry, *Sep. Purif. Technol.*, **76**: 345-350 (2011).

[10] Kebir M., Chabani M., Nasrallah N., Bensmaili A., Trari M., Coupling Adsorption with Photocatalysis Process for the Cr(VI) Removal, *Desalination,* **270**: 166-173 (2011).

[11] Colón G., Hidalgo M.C., Navío J.A., Photocatalytic Deactivation of Commercial TiO_2 Samples During Simultaneous Photoreduction of Cr(VI) and Photooxidation of Salicylic Acid, *J. Photochem. Photobiol., A,* **138**: 79-85 (2001).

[12] Giménez J., Aguado M.A., Cervera-March S., Photocatalytic Reduction of Chromium (VI) with Titania Powders in a Flow System. Kinetics and Catalyst Activity, *J. Mol. Catal. A: Chem.*, **105**: 67-78 (1996).

[13] Navío J.A., Colón G., Trillas M., Peral J., Domenech X., Testa J.J., Padron J., Rodríguez D., Litter M.I., Heterogeneous Photocatalytic Reactions of Nitrite Oxidation and Cr(VI) Reduction on Iron-Doped Titania Prepared by the Wet Impregnation Method. *Appl. Catal., B,* **16**:187-196 (1998).

[14] Ming Ma C., Shuen Shen Y., Hsiang Lin P., Photoreduction of Cr(VI) Ions in Aqueous Solutions by UV/TiO_2 Photocatalytic Processes, *Int. J. Photoenergy*, **2012**: 1-7 (2012).

[15] Nabizadeh R., Jahangiri Rad M., Nitrate Adsorption by Pan-Oxime-Nano Fe_2O_3 Using a Two-Level Full Factorial Design, *Research Journal of Nanoscience and Nanotechnology*, **6**: 1-7 (2016).

[16] Özgür Ü., Alivov Ya.I., Liu C., Teke A., Reshchikov M.A., Doğan S., Avrutin V., Cho S.-J., Morkoç H., A Comprehensive Review of ZnO Materials and Devices. *J. Appl. Phys.*, **98**(4): 041301 (2005).

[17] Manavizadeh N., Khodayari A.R., Asl Soleimani A., Bagherzadeh S., A Study of ZnO Buffer Layer Effect on Physical Properties of ITO Thin Films Deposited on Different Substrates, *Iran. J. Chem. Chem. Eng. (IJCCE),* **31**: 37-42 (2012).

[18] Al-Dahash G., Mubdir Khilkala W., Abdul Vahid S.N., Preparation and Characterization of ZnO Nanoparticles by Laser Ablation in NaOH Aqueous Solution, *Iran. J. Chem. Chem. Eng.(IJCCE),* **37**:11-16 (2018).

[19] Al-Sagheer F.A., Zaki M.I., Synthesis and Surface Characterization of Todorokite-type Microporous Manganese Oxides: Implications for Shape-Selective Oxidation Catalysts, *Microporous Mesoporous Mater.*, **67**: 43–52 (2004).

[20] Alanis C., Natividad R., Barrera-Diaz C., Martinez-Miranda V., Prince J., Valente J.S., Photocatalytically Enhanced Cr(VI) Removal by Mixed Oxides Derived from Me Al (Me: Mg and/or Zn) Layered Double Hydroxides, *Appl. Catal., B*, **140**: 546-551 (2013).

[21] Cai X., Cai Y., Liu Y., Deng S., Wang Y., Wang Y., Djerdj I., Photocatalytic Degradation Properties of $Ni(OH)_2$ Nanosheets/ZnO Nanorods Composites for Azo Dyes under Visible-Light Irradiation, *Ceram. Int.*, **40**:57-65 (2014).

[22] Sudeepan J., Kumar K., Barman T.K., Sahoo, P., Study of Friction and Wear of ABS/ZnO Polymer Composite Using Taguchi Technique, *Procedia Materials Science*, **6**: 391-400 (2014).

[23] Ross P.J., "Taghuchi Techniques for Quality Engineering", McGraw-Hill, New York, (1998).

[24] Donmez B., Celik C., Colak S., Yartas¸ A., Dissolution Optimization of Copper from Anode Slime in H_2SO_4 Solutions, *Ind. Eng. Chem. Res.*, **37**: 3382-3387 (1998).

[25] Copur M., Pekdemir T., Celik C., Colak, S., Determination of the Optimum Conditions for the Dissolution of Stibnite in HCl Solutions. *Ind. Eng. Chem. Res.*, **36**: 682-687 (1997).

[26] Khoei A.R., Masters I. Gethin D.T., Design Optimisation of Aluminium Recycling Processes Using Taguchi Technique, *J. Mater. Process. Technol.*, **127**: 96-106 (2002).

[27] Tortum A., Celik C., Aydin A.C., Determination of the Optimum Conditions for Tire Rubber in Asphalt Concrete, *Build. Environ.*, **40**: 1492-1504 (2005).

[28] Balakhonov S.V., Churagulov B.R., Gudilin E.A., Selective Cleaning of Ions of Heavy Metals from Water Solutions Using the H-form of Todorokite Synthesized by the Hydrothermal Method, *J. Surf. Invest.*, **2**:152-155 (2008).

[29] Jin Z., Zhang Y.X., Meng F.L., Jia Y., Luo T., Yu X.Y., Wang J., Liu J.H., Huang X.J., Facile Synthesis of Porous Single Crystalline ZnO Nanoplates and their Application in Photocatalytic Reduction of Cr(VI) in the Presence of Phenol. *J. Hazard. Mater.*, **276**: 400-407 (2014).

[30] Chakrabarti S., Chaudhuri B., Bhattacharjee S., Ray A.K., Dutta B.K., Photo-Reduction of Hexavalent Chromium in Aqueous Solution in the Presence of Zinc Oxide as Semiconductor Catalyst, *Chem. Eng. J.*, **153**: 86-93 (2009).

[31] Kabra K., Chaudhary R., Sawhney, R.L., Treatment of Hazardous Organic and Inorganic Compounds through Aqueous-Phase Photocatalysis: A Review. *Ind. Eng. Chem. Res.*, **43**: 7683-7696 (2004).

[32] Wang S., Wang Z., Zhuang Q., Photocatalytic Reduction of the Environmental Pollutant Cr^{VI} Over a Cadmium Sulphide Powder under Visible Light Illumination, *Appl. Catal., B*, **1**: 257–270 (1992).

[33] Mehrotra k., Yablonsky G.S., Ray A.K., Macro Kinetic Studies for Photocatalytic Degradation of Benzoic Acid in Immobilized Systems, *Chemosphere*, **60**: 1427-1436 (2005).